—Original—

Incidence of spontaneous lymphomas in non-experimental NOD/Shi-*scid*, IL-2Rγ^{null} (NOG) mice

Masahiko YASUDA[1], Tomoyuki OGURA[2], Takayuki GOTO[3], Mika YAGOTO[1], Yoko KAMAI[1], Chie SHIMOMURA[3], Nobuhito HAYASHIMOTO[4], Yukito KIYOKAWA[3], Hideki SHINOHARA[3], Riichi TAKAHASHI[2], and Kenji KAWAI[1]

[1]*Pathology Analysis Center, Central Institute for Experimental Animals (CIEA), 3-25-12 Tonomachi, Kawasaki-ku, Kawasaki, Kanagawa 210-0821, Japan*
[2]*Animal Resources Center, Central Institute for Experimental Animals (CIEA), 3-25-12 Tonomachi, Kawasaki-ku, Kawasaki, Kanagawa 210-0821, Japan*
[3]*Technical Service Department, CLEA Japan, Inc., 4839-23 Kitayama, Fujinomiya, Shizuoka 418-0112, Japan*
[4]*ICLAS Monitoring Center, Central Institute for Experimental Animals (CIEA), 3-25-12 Tonomachi, Kawasaki-ku, Kawasaki, Kanagawa 210-0821, Japan*

Abstract: Severely immunodeficient NOD/Shi-*scid*, IL-2Rγ^{null} (NOG) mice provide an *in vivo* model for human cell/tissue transplantation studies. NOG mice were established by combining interleukin-2 receptor-γ chain knockout mice and NOD/Shi-*scid* mice. They exhibit a high incidence of thymic lymphomas and immunoglobulin (Ig) leakiness. In this study, we assessed the incidence of malignant lymphomas and the occurrence of leakiness in 2,184 non-experimental NOG retired breeder mice aged 16–40 weeks. We established that the total incidence of lymphomas was only 0.60% (13/2,184). Most lymphomas (10/13) occurred in female mice by the age of around 25 weeks. No mice developed Ig leakiness. All lymphomas were derived from the thymus, and consisted mainly of CD3-positive and CD45R-negative lymphoblastic-like cells. Therefore, based on the absence of Ig leakiness and a very low incidence of lymphomas, including thymic lymphomas, NOG mice may be useful in regeneration medicine for xenotransplantation of human embryonic stem (ES) cells or induced pluripotent stem (iPS) cells, and in transplantation experiments involving tumor cells.
Key words: NOG mouse, thymic lymphoma

Introduction

NOD/Shi-*scid*, IL-2Rγ^{null} (NOG; formally NOD. Cg-*Prkdc^{scid} Il2rg$^{tm1 Sug}$*/ShiJic) mice are severely immuno-deficient and are used as *in vivo* models for human cell/tissue transplantation studies [9, 33]. Recently, NOG mice have been used to test tumorigenicity in induced pluripotent stem cell (iPSC)-derived cell products, including the first iPSC-derived retinal pigment epithelium cell sheet [16, 17]. Furthermore, various improved strains of NOG mice are excellent humanized mouse models

[12, 14, 28]. NOG mice were established by combining NOD/ShiJic-*Prkdc^{scid}* (NOD-*scid*) mice and interleukin (IL)-2 receptor-γ chain knockout mice. As a result, NOG mice present defects in T-, B-, and natural killer cells, as well as poorly functioning macrophages and dendritic cells [11]. NOD-*scid* mice show a high incidence of thymic lymphomas, and some mice develop partial immune reactivity termed "leakiness," despite the absence of T- and B-cells in normal NOD-*scid* mice [2, 22, 27]. NOG mice share the genetic background of NOD-*scid* mice, and can develop thymic lymphomas and leakiness.

Kato *et al.* reported an extremely low incidence of thymic lymphomas in NOG mice [15]. This is in spite of several of those mice being pretreated with irradiation, a known inducer of mouse thymic lymphoma [31], before xenotransplantion. Additionally, the occurrence of leakiness could not be clearly established in NOG mice with thymic lymphomas [15]. In contrast, Katano *et al.* reported no leakiness and no incidence of thymic lymphomas in NOG mice [13], however, their study included only a small number of mice. So far, no report has described the incidence of tumors other than lymphomas in NOG and NOD-*scid* mice, and little information is available on spontaneous non-lymphomatous tumors even in CB17/Icr-*Prkdc^scid* (CB17-*scid*) mice [4, 10]. Therefore, here, we evaluated the incidence of spontaneous tumors including thymic lymphomas and the occurrence of leakiness in non-experimental NOG mice. At the same time, this is the first report of spontaneous non-lymphomatous tumors in NOG mice.

Materials and Methods

Animals

All NOG mice used in this study were bred and maintained in the production colony at CLEA Japan, Inc. (Fujinomiya, Japan), and were housed in an exclusive specific-pathogen-free room fitted with a bioBubble™ (bioBUBBLE, Inc., Fort Collins, CO, USA). The animal room was maintained at $24 \pm 2°C$ with $55 \pm 15\%$ relative humidity and with a 12-h light/dark cycle. All mice were fed an autoclaved (127°C, 30 min) CL-2 diet (CLEA Japan, Inc., Tokyo, Japan) and provided *ad libitum* access to autoclaved (127°C, 30 min) tap water. The mouse facility of CLEA Japan, Inc. is accredited by the Association for Accreditation and Assessment for Laboratory Animal Care and Use International.

To investigate the incidence of spontaneous lymphomas, non-experimental retired NOG mice were necropsied, because retired breeder mice are commonly used for aging or cancer studies. A total of 2,184 retired NOG mice (1,043 males and 1,141 females) were examined at weekly intervals. Their age ranged from 16 to 40 weeks (16–20, 21–25, 26–30, 31–40 weeks), with the average age of examined male and female mice being 26.6 and 27.6 weeks, respectively. Retired breeders included breeding male/female mice that had been sterile for two months, and old breeding males/females that had lived for longer than eight months after the first mating.

Complete necropsies were performed on all retired NOG breeders every week over a seven-months surveillance period. Mice were euthanized by exsanguination under isoflurane anesthesia and then necropsied. To determine serum Ig levels, blood samples (minimum of 0.2 ml of whole blood) were collected from the caudal vena cava or the heart. Sera were separated by centrifugation (2,500 rpm, 5 min) and the resulting serum samples were stored at −20°C. Organs such as the thymus and spleen were weighted.

Single radial immunodiffusion (SRID)

To determine the presence of immunoglobulin leakiness in NOG mice with an enlarged thymus, serum Ig levels were assayed by SRID [19], using plates containing agarose gel incorporating anti-mouse IgG, IgA, and IgM (Medical & Biological Laboratories CO., LTD., Nagoya, Japan). A serum sample (10 μl) was added to each well, the agar plates were incubated for 48 h at 25°C, and the diameter of the precipitin rings was measured to the nearest 0.1 mm. The detection limit was estimated to be 2.3 μg/ml, as determined using reference serum. Positive control serum was obtained from normal Jcl:ICR mice.

Histopathological analysis and immunohistochemistry

To determine the presence of lymphomas, the thymus, spleen, bone marrow of the sternum, and other organs with metastatic lesions associated with lymphoma, as well as organs with visible abnormal lesions unrelated to lymphoma, were collected in 10% neutral-buffered formalin, embedded in paraffin, and sectioned into 4-μm-thick slices. These were stained with hematoxylin and eosin (HE) for histopathological examination by light microscopy. To diagnose thymic neoplasms, immunohistochemical staining was performed as instructed by the manufacturer using a Leica BOND-MAX automated IHC/ISH stainer and a Leica Refine detection kit (Leica Biosystems K.K., Tokyo, Japan). Sections were incubated with primary antibodies diluted with Bond Primary Antibody Diluent (Leica Biosystems), as detailed in Table 1. The pathological evaluation of lymphoid organs, such as the thymus, spleen, and bone marrow, was performed according to the "STP Position Paper" published by the STP Immunotoxicity Working Group [8] and "A Monograph on Histopathologic Evaluation of Lymphoid Organs [20]."

Table 1. Protocol used for each primary antibody

Antibody	Host	Clone	Dilution	Antigen retrieval	Source[d]
Cleaved caspase-3 (Asp175)	Rabbit	Polyclonal	1:1,500	ER2[a]	Cell Signaling Technology
CD3	Rabbit	SP7	1:50	ER1[b]	Nichirei
mCD45R (B220)	Rat	RA3-6B2	1:200	ER1[b]	Santa Cruz Biotechnology
Ki-67	Rabbit	SP6	1:100	ER2[a]	Abcam
Keratin/Cytokeratin	Rabbit	Polyclonal	1:1	Protease[c]	Nichirei

[a]Treated with ER2 (EDTA-based pH9.0 epitope retrieval solution; Leica Biosystems K.K., Tokyo, Japan) for 20 min at 100°C. [b]Treated with ER1 (Citrate-based pH6.0 epitope retrieval solution; Leica Biosystems) for 30 min at 100°C. [c]Treated with Protease Solution (Prediluted; Nichirei Biosciences, Inc., Tokyo, Japan) for 5 min at room temperature. [d]Sources: Cell Signaling Technology, Inc. (Danvers, MA, USA), Nichirei Biosciences, Inc., Santa Cruz Biotechnology, Inc. (Dallas, TX, USA), Abcam plc (Cambridge, UK).

Results

Occurrence and incidence of thymic enlargement in NOG mice

As shown in Table 2, the total incidence of visibly enlarged thymuses was 0.60% (13/2,184) in all NOG retired breeders, 0.29% (3/1,043) in male mice, and 0.88% (10/1,141) in female mice. In particular, enlarged thymus tended to occur in females by 25 weeks of age, with an incidence of 1.84% (9/490), as compared to same-age males (0.39%, 2/510).

Serum Ig assay

IgG, IgA, and IgM could not be detected by SRID in NOG mice with an enlarged thymus.

Gross and histopathological lesions

Necropsy revealed that in normal NOG mice, the thymus was located in the anterior mediastinum and superior to the heart, a position typical of immunocompetent and other immunodeficient mouse strains (Fig. 1). However, the thymus had undergone so-called "thymic atrophy," being only about 0.1 cm in size, such that its weight was difficult to measure exactly (average weight of the normal thymus was approximately 5–20 mg). Moreover, the thymus was buried in periaortic adipose tissue, which made it difficult to see by eye. The normal spleen was also small: absolute weight was 49 ± 25 mg and relative weight was 172 ± 83 mg/100 g body weight (mean ± SD). Finally, the normal lymph node was also remarkably small. Abnormal NOG mice with enlarged thymuses showed clinical signs of weakening, such as a hunchback position, anemia, and weight loss (average body weight was 21.0 ± 2.2 g). The abnormal enlarged thymuses were generally of a white or light-brown

Table 2. Occurrence and incidence of visibly enlarged thymuses in NOG mice

Age range (weeks)	Males (%)	Females (%)
16–20	0/331 (0.00)	8/310 (2.58)
21–25	2/179 (1.12)	1/180 (0.56)
26–30	1/191 (0.52)	0/207 (0.00)
31–40	0/342 (0.00)	1/444 (0.23)
16–40	3/1043 (0.29)	10/1,141 (0.88)

Results are given as the number of mice presenting thymic enlargement/number of examined mice.

color with lobular structures: absolute weight was 336 ± 325 mg and relative weight was $1,579 \pm 1,517$ mg/100 g body weight. Severely enlarged thymuses were seen to occupy most of the thoracic cavity with associated pleural effusion and/or ascites, and adhered to the pleura, heart, and lungs (Fig. 1). As shown in Table 3, three out of 13 abnormal NOG mice presented only visibly enlarged thymuses, whereas others revealed also enlarged spleen, lung subinvolution with red or brick-red discoloration, enlarged liver, and/or enlarged lymph nodes. The absolute weight of the enlarged spleen was 173 ± 139 mg and relative weight was 828 ± 639 mg/100 g body weight. Finally, in NOG mice with severely enlarged thymuses, whitish neoplastic tissue/cells were seen to invade the mediastinum and pleural effusion.

A histopathological examination revealed that in normal NOG mice, the thymus and spleen were hypoplastic. Normal thymuses were devoid of lymphoid cells and cortico-medullary junctions, and consisted mostly of thymic epithelial and stromal cells (Fig. 2). Thymic epithelial cells were immunohistochemically positive for cytokeratin (Fig. 2). Some NOG mice presented non-neoplastic lesions of the thymus, such as sporadic cystic structures, ectopic exocrine glands, and ectopic parathy-
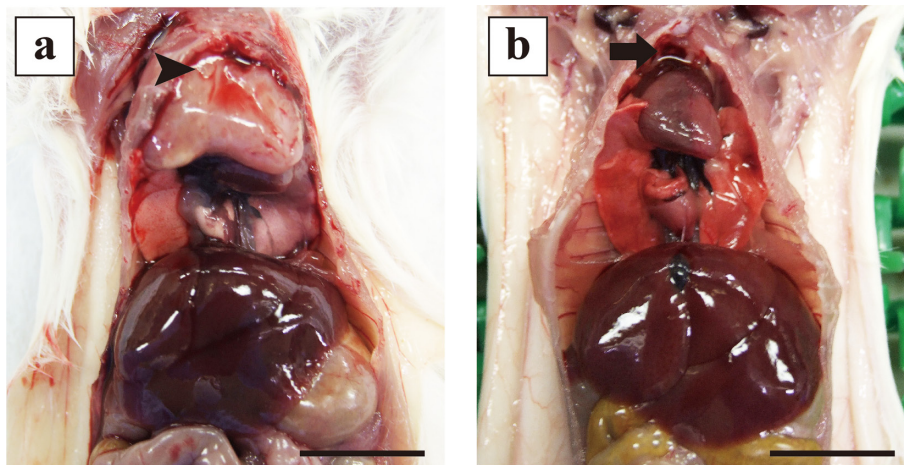
Fig. 1. Gross appearance of an enlarged thymus from a female NOG mouse aged 16–20 weeks (A), compared with a that from a same-age normal female NOG mouse (B). A: The enlarged thymus (arrowhead) is seen to occupy most of the thoracic cavity with lung hepatization and pleural effusion. B: The normal thymus is very small and buried in periaortic adipose tissue (arrow). Bars: 1 cm.
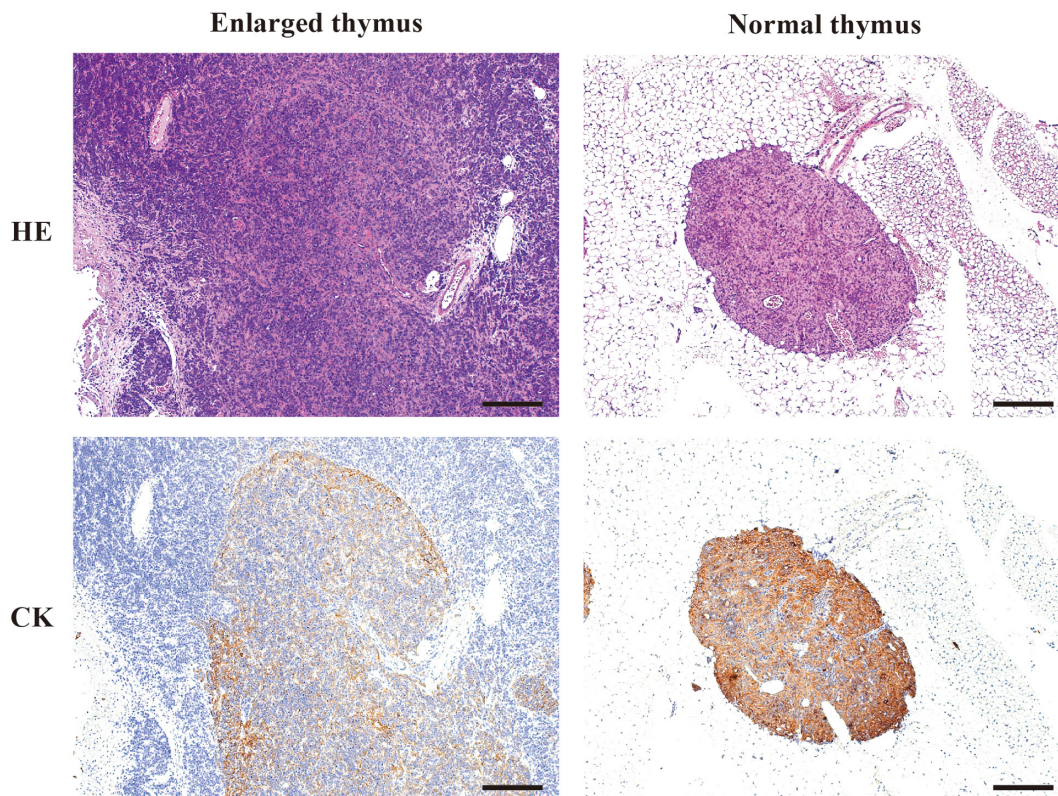

Fig. 2. Histopathological and immunohistochemical analysis of an enlarged thymus from a female NOG mouse (Fig. 1) and a normal thymus from a normal female NOG mouse. The normal thymus shows severe hypoplasia and mostly cytokeratin (CK)-positive thymic epithelial cells. In the enlarged thymus, CK-negative neoplastic cells show invasion to the CK-positive thymic epithelial meshwork structure. Bars: 200 μm.

Table 3. Characterization of the NOG mice with an enlarged thymus

Case	Age range (weeks)	Sex	Clinical symptoms	Necropsy finding	Body weight (g)	Thymus weight (mg)	Spleen weight (mg)
1	16–20	Female	Weakening and anemic response	Enlarged thymus	21.2	148	16
2	16–20	Female	Weakening and anemic response	Enlarged thymus and spleen	21.3	105	102
3	16–20	Female	Wasting	Enlarged thymus and spleen Swollen lungs and liver Pleural effusion	20.3	436	428
4	16–20	Female	Weakening and anemic response	Enlarged thymus Lung hepatization Pleural effusion Ascitic fluid	23.4	162	51
5	16–20	Female	No change	Enlarged thymus	22.7	41	55
6	16–20	Female	Weakening and anemic response	Enlarged thymus and spleen Pleural effusion	21.4	184	204
7	16–20	Female	Weakening and anemic response	Enlarged thymus Lung hepatization Pleural effusion	21.5	529	79
8	16–20	Female	Wasting	Enlarged thymus and spleen	15.2	40	125
9	21–25	Male	Wasting	Enlarged thymus and spleen	19.6	173	208
10	21–25	Male	Wasting	Enlarged thymus, spleen and intrathoracic lymph nodes Pleural effusion	22.0	240	111
11	21–25	Female	Wasting	Enlarged thymus, spleen, and intrathoracic lymph nodes Lung hepatization Swollen liver and kidney Pleural effusion Ascitic fluid	21.1	1,202	322
12	26–30	Male	Anemic response	Enlarged thymus and spleen	24.0	657	431
13	31–40	Female	Wasting	Enlarged thymus and spleen Lung hepatization Pleural effusion	19.6	454	120

roid glands. Normal spleens revealed absence of lymphoid cell follicles, with some presenting osseous metaplasia and/or extramedullary hematopoiesis (Fig. 4). Normal NOG mice presented neither CD3- nor CD45R-positive lymphocytes in the thymus (Fig. 3), spleen (Fig. 4), or bone marrow.

All enlarged thymuses consisted mainly of neoplastic lymphoblastic cells. The neoplastic lymphocytes invaded the thymic capsule and neighboring adipose tissue. As a result, the cytokeratin-positive thymic epithelial meshwork structure was destroyed and surrounded by neoplastic cell sheets (Fig. 2). The neoplastic lymphocytes were non-cohesive, medium-sized with scant and deeply basophilic cytoplasm (Fig. 3). Their nuclei were round to pleomorphic, with hypochromatin and promi-

nent nucleoli. Moreover, cells exhibited numerous mitoses and homogeneous sheet-like growth. Scattered macrophages with a 'starry sky' appearance were observed among neoplastic cell sheets. All neoplastic lymphocytes in enlarged thymuses were cytoplasmic CD3-positive (Fig. 3), CD45R-negative (Fig. 3), and cytokeratin-negative, with most of the CD3-positive cells being also positive for Ki-67. As CD3-positive cells were retained within the thymic mass, neoplastic lymphocytes were considered to be of T-cell origin. At the same time, the normal/enlarged thymus and spleen were characterized by CD45R-positive small-sized cells. However, these CD45R-positive cells presented small, apoptotic, deeply staining nuclei, and were caspase-3-positive.
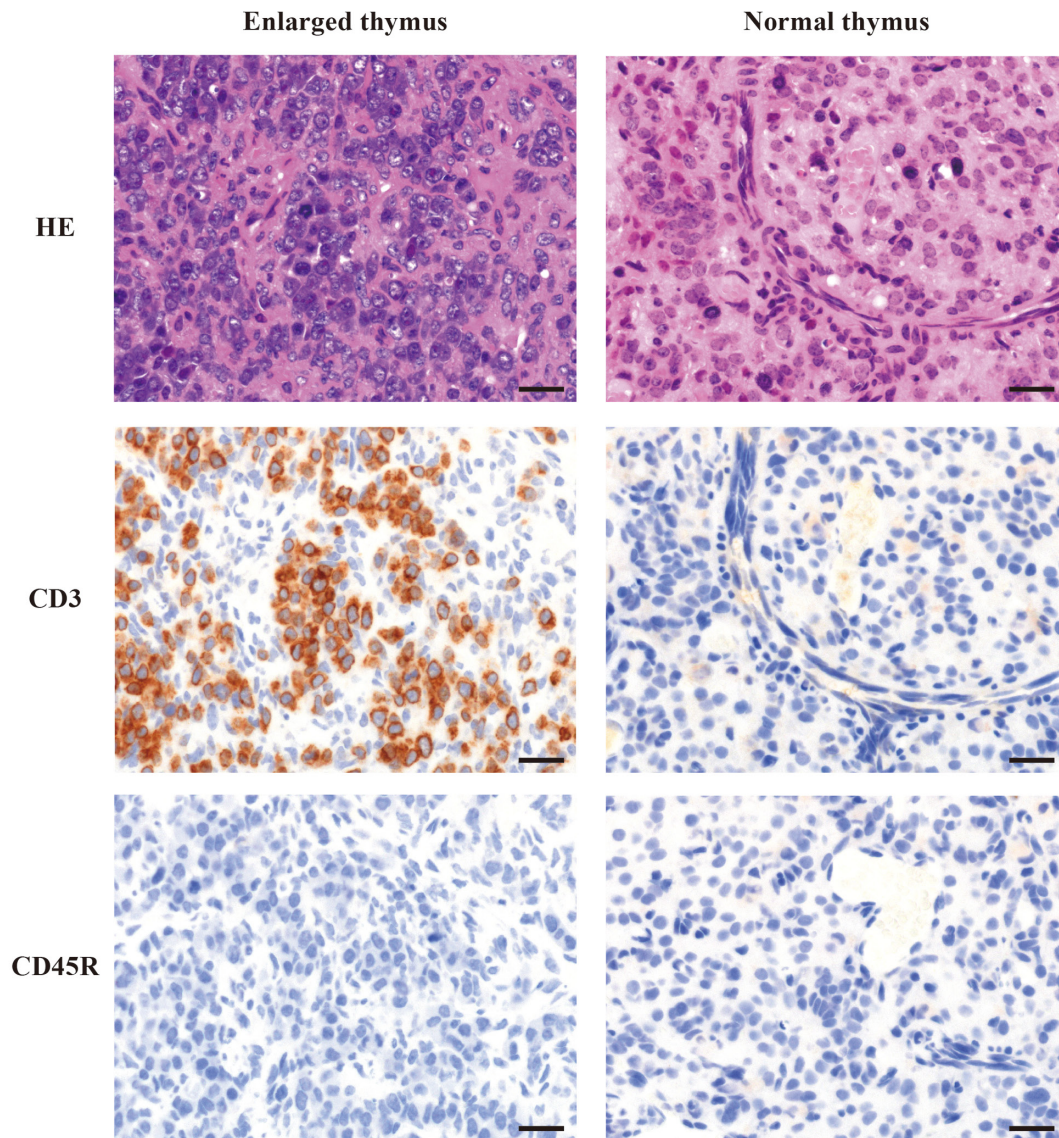
Neoplastic lymphocytes were seen to spread into me-

	Enlarged thymus	**Normal thymus**
HE		
CD3		
CD45R		

Fig. 3. Histopathological and immunohistochemical analysis of an enlarged thymus and a normal one. High magnification of Fig. 2. In the normal thymus, thymic epithelial cells appear negative for CD3 and CD45R. In the enlarged thymus, CD3-positive and CD45R-negative neoplastic cells show monomorphous proliferation. Bars: 20 μm.

diastinal tissue adjacent to the enlarged thymus. In ten out of 13 NOG mice with an enlarged thymus, invading CD3-positive and CD45R-negative neoplastic lymphocytes were observed also in adjacent and intraperitoneal organs, such as the lungs, heart, aorta, esophagus, trachea, upper thoracic vertebrae, spleen, liver, and kidney. In the enlarged spleen, CD3-positive lymphoma cells were found in the white pulp, infiltrating the red pulp, or expanded diffusely (Fig. 4). In the lungs, they bilaterally invaded the perivascular and peribronchial region, or expanded diffusely (Fig. 5). In the heart, they invaded

the pericardium, myocardial intestinal tissue, and peri-aortic and precaval adipose tissue. In the liver, CD3-positive lymphoma cells infiltrated the hepatic sinusoids and triad areas (Fig. 5). In the kidney, they infiltrated the renal interstitium (Fig. 5). Finally, as these metastatic cells were CD3-positive and CD45R-negative, they were assumed to derive from T-cells in the thymus.

During the same period, spontaneous non-lymphomatous neoplastic lesions were detected only in female NOG mice, with an incidence of 0.44% (5/1,141), as compared to 0.23% (5/2,184) in all NOG retired breed-
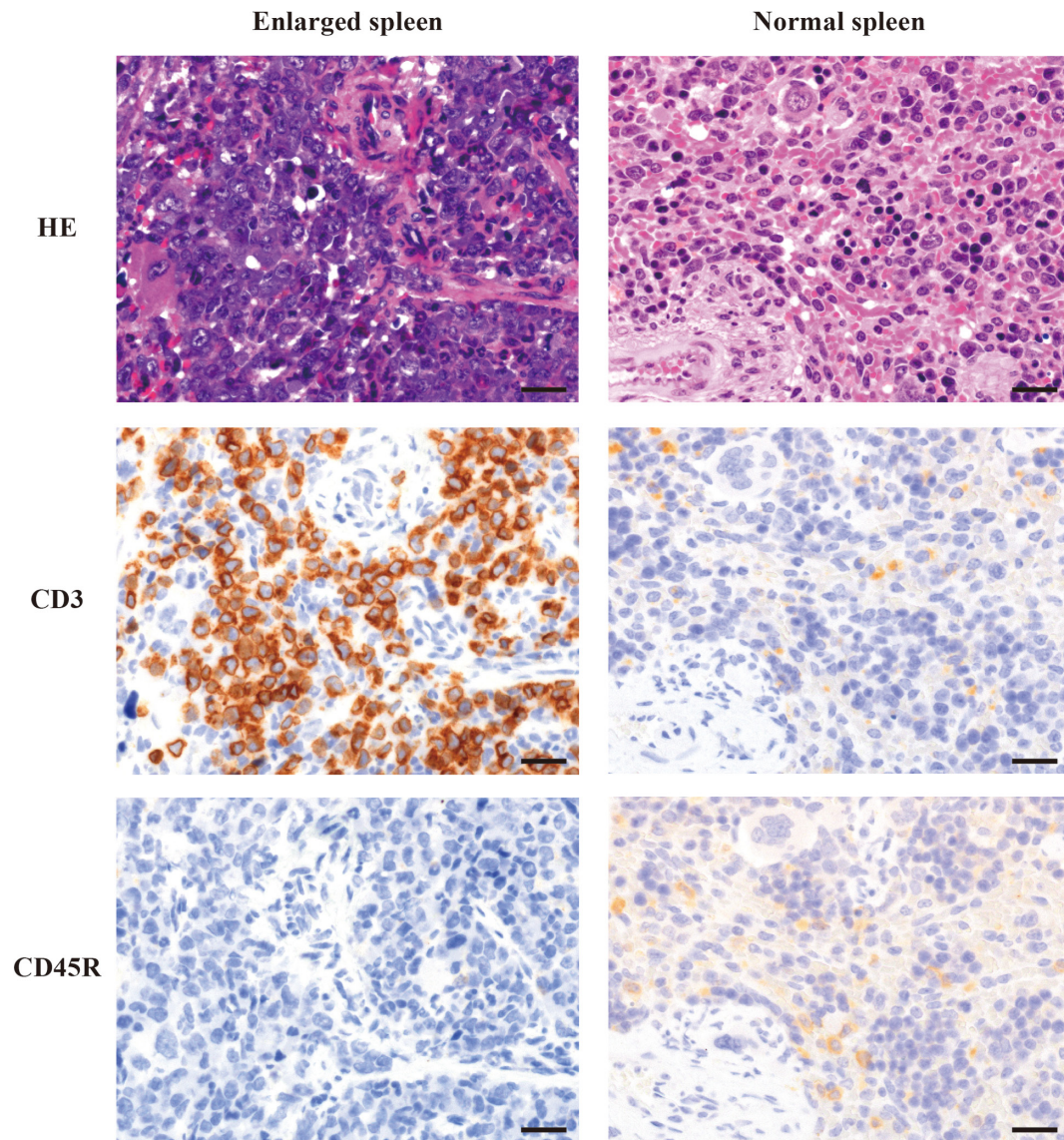
	Enlarged spleen	**Normal spleen**

Fig. 4. Representative histopathological features of an enlarged spleen in a NOG mouse with an enlarged thymus (Figs. 2 and 3) compared with a normal spleen. Neither CD3- nor CD45R-positive lymphocytes are observed in the normal spleen with extramedullary hematopoiesis. In the enlarged spleen, as well as in the enlarged thymus, CD3-positive and CD45R-negative neoplastic lymphocytes infiltrate into the perivascular lymphoid sheath in the white pulp. Bars: 200 μm.

ers (Table 4).

From the above results, spontaneous tumors including thymic lymphomas were detected with an incidence of 0.82% (18/2,184) in all NOG mice, 0.29% (3/1,043) in male mice, and 1.31% (15/1,141) in female mice. Therefore, in NOG mice, thymic lymphoma has the highest incidence among spontaneous tumors.

Discussion

To our knowledge, there are only a few reports about the development of lymphomas and Ig leakiness in NOG mice [13, 15]. In the present study, we investigated the incidence of spontaneous lymphomas in untreated and non-irradiated NOG mice. We based our choice on reports of non-irradiated NOG mice surviving longer than irradiated mice prior to transplantation with human stem cells [32], and of radiation inducing mouse lymphomas
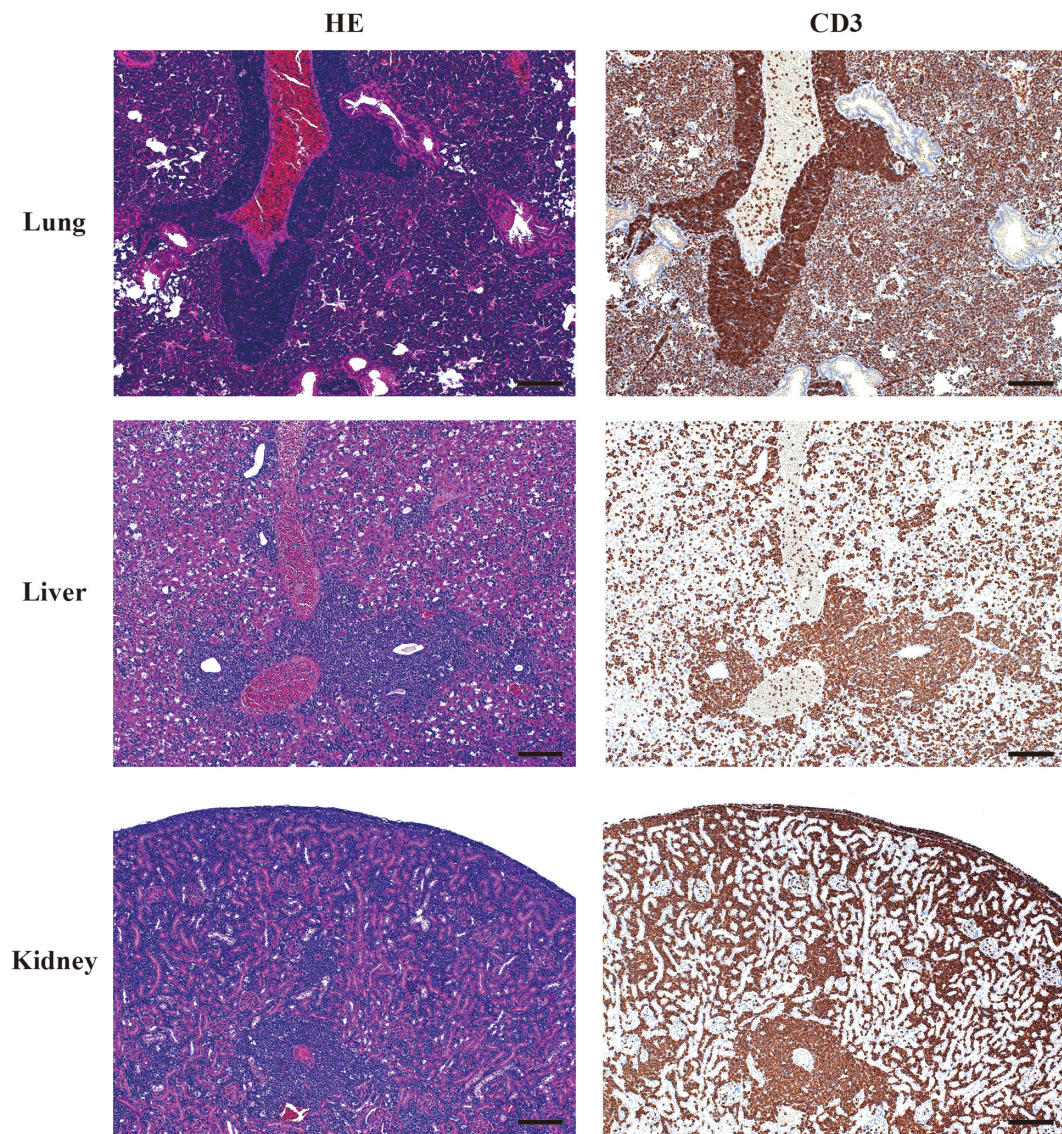
HE	CD3

Fig. 5. Photomicrograph of neoplastic cells invading the lungs, liver, and kidneys of a female NOG mice aged 21–25 weeks. CD3-positive neoplastic cells invade the perivascular regions and expand diffusely. Bars: 200 μm.

Table 4. Characterization of non-lymphomatous tumors in NOG mice

Case	Age range (weeks)	Sex	Clinical symptoms	Necropsy finding	Diagnosis
1	21–25	Female	None	The right lower abdominal subcutaneous mass in the region of the mammary gland	Adenocarcinoma [26]
2	26–30	Female	None	Enlargement of the left ovary	Teratoma, benign [5]
3	26–30	Female	None	Nodular lesion in the right lower lobe of the lung	Carcinoma, bronchiolo-alveolar [23]
4	31–40	Female	None	Retroperitoneal mass	Rabdomyosarcoma [7]
5	31–40	Female	None	The left lower abdominal subcutaneous mass in the region of the mammary gland	Adenoma [26]

[3]. Overall, the incidence of lymphomas was very low. Moreover, NOG mice with lymphomas did not develop any leakiness. Therefore, this and previous [15] reports confirm that NOG mice are resistant to lymphoma/leukemia development even after irradiation treatment.

Lymphomas are the most noticeable hematolymphoid tumors; however, the mechanism by which they occur in mice is unclear. Various factors, including retroviruses [30], irradiation [1, 3], and chemicals [6], can induce lymphomas/leukemia in mouse strains. In NOD-*scid* mice, whose genetic background is shared by NOG mice, endogenous ecotropic provirus *Emv30* is thought to be one of the causative agents of lymphomas [27]. Some immunodeficient mouse strains are characterized by the early activation of endogenous retroviruses [18, 34, 35]. Accordingly, immunocompromised NOD-*scid* mice are thought to activate *Emv30* and develop thymic lymphomas at a young age [27]. Additionally, Shultz *et al.* have suggested that the development of lymphomas in NOD-*scid* mice is dependent on cytokine signaling through the IL-2 receptor-γ chain [29]. Unlike NOD-*scid* mice, NOG mice lack the IL-2 receptor-γ chain, which may explain the low incidence of lymphomas and the absence of Ig leakiness observed in the present study.

At the same time, the incidence of spontaneous non-lymphomatous tumors (mammary gland adenoma/adenocarcinoma, teratoma, bronchiolo-alveolar carcinoma, and rabdomyosarcoma) was 0.23% in all NOG retired breeders, 0.00% in male mice, and 0.44% in female mice. In comparison, in CB17-*scid* mice (10–65 weeks of age), the total incidence of non-lymphomatous tumors is 1.5–1.9% [4, 10].

From the above results, and the macro- and micro-pathological characterization of lymphomas in 13 NOG mice, it can be concluded that: 1) lymphomas were primarily of thymic origin, 2) they occurred by about 25 weeks of age, 3) they consisted mainly of lymphoblastic neoplastic cells, 4) neoplastic lymphocytes were non-cohesive and medium-sized with scant cytoplasm, 5) neoplastic lymphocytes were cytoplasmic CD3-positive and CD45R-negative, and 6) CD3-positive and CD45R-negative metastatic cells invaded the perivascular regions of the spleen, lung, liver, and kidney. CD45R-positive small-sized cells were observed in the normal/enlarged thymus and the spleen. However, these CD45R-positive cells presented small, apoptotic, deeply staining nuclei, and were caspase-3-positive. Therefore, given that the CD45R epitope was reported to be expressed on

T-cells or thymocytes undergoing apoptosis [21, 24, 25], these cells were considered apoptotic cells and not B-cells. Consequently, we speculate that lymphomas in young NOG mice were thymus-derived T-cell lymphoblastic lymphomas. In summary, unlike SCID mice, the absence of Ig leakiness and a very low incidence of spontaneous tumors, including lymphomas, make NOG mice a useful model in xenotransplantation experiments, such as iPSC treatment studies.

References

1. Boorman, G.A., Rafferty, C.N., Ward, J.M., and Sills, R.C. 2000. Leukemia and lymphoma incidence in rodents exposed to low-frequency magnetic fields. *Radiat. Res.* 153: 627–636. [Medline] [CrossRef]
2. Bosma, G.C., Fried, M., Custer, R.P., Carroll, A., Gibson, D.M., and Bosma, M.J. 1988. Evidence of functional lymphocytes in some (leaky) *scid* mice. *J. Exp. Med.* 167: 1016–1033. [Medline] [CrossRef]
3. Coggin, J.H. Jr., Rohrer, S.D., Leinbach, E.D., Hester, R.B., Liu, P.I., and Heath, L.S. 1988. Radiation-induced lymphoblastic lymphomas/leukemias and sarcomas of mice express conserved, immunogenic 44-kilodalton oncofetal antigen. *Am. J. Pathol.* 130: 136–146. [Medline]
4. Custer, R.P., Bosma, G.C., and Bosma, M.J. 1985. Severe combined immunodeficiency (SCID) in the mouse. Pathology, reconstitution, neoplasms. *Am. J. Pathol.* 120: 464–477. [Medline]
5. Dixon, D., Alison, R., Bach, U., Colman, K., Foley, G.L., Harleman, J.H., Haworth, R., Herbert, R., Heuser, A., Long, G., Mirsky, M., Regan, K., Van Esch, E., Westwood, F.R., Vidal, J., and Yoshida, M. 2014. Nonproliferative and proliferative lesions of the rat and mouse female reproductive system. *J. Toxicol. Pathol.* 27 (3–4 Suppl): 1S-107S. [Medline] [CrossRef]
6. Gold, L.S., Manley, N.B., Slone, T.H., and Ward, J.M. 2001. Compendium of chemical carcinogens by target organ: results of chronic bioassays in rats, mice, hamsters, dogs, and monkeys. *Toxicol. Pathol.* 29: 639–652. [Medline] [CrossRef]
7. Greaves, P., Chouinard, L., Ernst, H., Mecklenburg, L., Pruimboom-Brees, I.M., Rinke, M., Rittinghausen, S., Thibault, S., Von Erichsen, J., and Yoshida, T. 2013. Proliferative and non-proliferative lesions of the rat and mouse soft tissue, skeletal muscle and mesothelium. *J. Toxicol. Pathol.* 26:(Suppl): 1S–26S. [Medline] [CrossRef]
8. Haley, P., Perry, R., Ennulat, D., Frame, S., Johnson, C., Lapointe, J.M., Nyska, A., Snyder, P., Walker, D., Walter, G.,

STP Immunotoxicology Working Group. 2005. STP position paper: best practice guideline for the routine pathology evaluation of the immune system. *Toxicol. Pathol.* 33: 404–407, discussion 408. [Medline] [CrossRef]

9. Hiramatsu, H., Nishikomori, R., Heike, T., Ito, M., Kobayashi, K., Katamura, K., and Nakahata, T. 2003. Complete reconstitution of human lymphocytes from cord blood CD34+ cells using the NOD/SCID/gammacnull mice model. *Blood* 102: 873–880. [Medline] [CrossRef]

10. Huang, P., Westmoreland, S.V., Jain, R.K., and Fukumura, D. 2011. Spontaneous nonthymic tumors in SCID mice. *Comp. Med.* 61: 227–234. [Medline]

11. Ito, M., Hiramatsu, H., Kobayashi, K., Suzue, K., Kawahata, M., Hioki, K., Ueyama, Y., Koyanagi, Y., Sugamura, K., Tsuji, K., Heike, T., and Nakahata, T. 2002. NOD/SCID/γ(c) (null) mouse: an excellent recipient mouse model for engraftment of human cells. *Blood* 100: 3175–3182. [Medline] [CrossRef]

12. Ito, R., Takahashi, T., Katano, I., Kawai, K., Kamisako, T., Ogura, T., Ida-Tanaka, M., Suemizu, H., Nunomura, S., Ra, C., Mori, A., Aiso, S., and Ito, M. 2013. Establishment of a human allergy model using human IL-3/GM-CSF-transgenic NOG mice. *J. Immunol.* 191: 2890–2899. [Medline] [CrossRef]

13. Katano, I., Ito, R., Eto, T., Aiso, S., and Ito, M. 2011. Immunodeficient NOD-*scid* IL-2Rγ(null) mice do not display T and B cell leakiness. *Exp. Anim.* 60: 181–186. [Medline] [CrossRef]

14. Katano, I., Takahashi, T., Ito, R., Kamisako, T., Mizusawa, T., Ka, Y., Ogura, T., Suemizu, H., Kawakami, Y., and Ito, M. 2015. Predominant development of mature and functional human NK cells in a novel human IL-2-producing transgenic NOG mouse. *J. Immunol.* 194: 3513–3525. [Medline] [CrossRef]

15. Kato, C., Fujii, E., Chen, Y.J., Endaya, B.B., Matsubara, K., Suzuki, M., Ohnishi, Y., and Tamaoki, N. 2009. Spontaneous thymic lymphomas in the non-obese diabetic/Shi-*scid*, IL-2R γ (null) mouse. *Lab. Anim.* 43: 402–404. [Medline] [CrossRef]

16. Kanemura, H., Go, M.J., Shikamura, M., Nishishita, N., Sakai, N., Kamao, H., Mandai, M., Morinaga, C., Takahashi, M., and Kawamata, S. 2014. Tumorigenicity studies of induced pluripotent stem cell (iPSC)-derived retinal pigment epithelium (RPE) for the treatment of age-related macular degeneration. *PLoS One* 9: e85336. [Medline] [CrossRef]

17. Kawamata, S., Kanemura, H., Sakai, N., Takahashi, M., and Go, M.J. 2015. Design of a tumorigenicity test for induced pluripotent stem cell (iPSC)-derived cell products. *J. Clin. Med.* 4: 159–171. [Medline] [CrossRef]

18. Kozak, C.A. 2014. Origins of the endogenous and infectious laboratory mouse gammaretroviruses. *Viruses* 7: 1–26. [Medline] [CrossRef]

19. Mancini, G., Carbonara, A.O., and Heremans, J.F. 1965. Immunochemical quantitation of antigens by single radial immunodiffusion. *Immunochemistry* 2: 235–254. [Medline] [CrossRef]

20. Maronpot, R.R. 2006. A monograph on histomorphologic evaluation of lymphoid organs. *Toxicol. Pathol.* 34: 407–

21. Oka, S., Mori, N., Matsuyama, S., Takamori, Y., and Kubo, K. 2000. Presence of B220 within thymocytes and its expression on the cell surface during apoptosis. *Immunology* 100: 417–423. [Medline] [CrossRef]

22. Prochazka, M., Gaskins, H.R., Shultz, L.D., and Leiter, E.H. 1992. The nonobese diabetic scid mouse: model for spontaneous thymomagenesis associated with immunodeficiency. *Proc. Natl. Acad. Sci. USA* 89: 3290–3294. [Medline] [CrossRef]

23. Renne, R., Brix, A., Harkema, J., Herbert, R., Kittel, B., Lewis, D., March, T., Nagano, K., Pino, M., Rittinghausen, S., Rosenbruch, M., Tellier, P., and Wohrmann, T. 2009. Proliferative and nonproliferative lesions of the rat and mouse respiratory tract. *Toxicol. Pathol.* 37:(Suppl): 5S–73S. [Medline] [CrossRef]

24. Renno, T., Attinger, A., Rimoldi, D., Hahne, M., Tschopp, J., and MacDonald, H.R. 1998. Expression of B220 on activated T cell blasts precedes apoptosis. *Eur. J. Immunol.* 28: 540–547. [Medline] [CrossRef]

25. Renno, T., Hahne, M., Tschopp, J., and MacDonald, H.R. 1996. Peripheral T cells undergoing superantigen-induced apoptosis *in vivo* express B220 and upregulate Fas and Fas ligand. *J. Exp. Med.* 183: 431–437. [Medline] [CrossRef]

26. Rudmann, D., Cardiff, R., Chouinard, L., Goodman, D., Küttler, K., Marxfeld, H., Molinolo, A., Treumann, S., Yoshizawa, K., INHAND Mammary, Zymbal's, Preputial, and Clitoral Gland Organ Working Group. 2012. Proliferative and nonproliferative lesions of the rat and mouse mammary, Zymbal's, preputial, and clitoral glands. *Toxicol. Pathol.* 40:(Suppl): 7S–39S. [Medline] [CrossRef]

27. Serreze, D.V., Leiter, E.H., Hanson, M.S., Christianson, S.W., Shultz, L.D., Hesselton, R.M., and Greiner, D.L. 1995. *Emv30*null NOD-*scid* mice. An improved host for adoptive transfer of autoimmune diabetes and growth of human lymphohematopoietic cells. *Diabetes* 44: 1392–1398. [Medline] [CrossRef]

28. Soulard, V., Bosson-Vanga, H., Lorthiois, A., Roucher, C., Franetich, J.F., Zanghi, G., Bordessoulles, M., Tefit, M., Thellier, M., Morosan, S., Le Naour, G., Capron, F., Suemizu, H., Snounou, G., Moreno-Sabater, A., and Mazier, D. 2015. Plasmodium falciparum full life cycle and Plasmodium ovale liver stages in humanized mice. *Nat. Commun.* 6: 7690. [Medline] [CrossRef]

29. Shultz, L.D., Lyons, B.L., Burzenski, L.M., Gott, B., Chen, X., Chaleff, S., Kotb, M., Gillies, S.D., King, M., Mangada, J., Greiner, D.L., and Handgretinger, R. 2005. Human lymphoid and myeloid cell development in NOD/LtSz-*scid IL2R γ null* mice engrafted with mobilized human hemopoietic stem cells. *J. Immunol.* 174: 6477–6489. [Medline] [CrossRef]

30. Taddesse-Heath, L., Chattopadhyay, S.K., Dillehay, D.L., Lander, M.R., Nagashfar, Z., Morse, H.C. 3rd., and Hartley, J.W. 2000. Lymphomas and high-level expression of murine leukemia viruses in CFW mice. *J. Virol.* 74: 6832–6837. [Medline] [CrossRef]

31. Wakabayashi, Y., Inoue, J., Takahashi, Y., Matsuki, A., Kosugi-Okano, H., Shinbo, T., Mishima, Y., Niwa, O., and Kominami, R. 2003. Homozygous deletions and point muta-

408. [Medline] [CrossRef]

tions of the *Rit1/Bcl11b* gene in γ-ray induced mouse thymic lymphomas. *Biochem. Biophys. Res. Commun.* 301: 598–603. [Medline] [CrossRef]

32. Watanabe, S., Ohta, S., Yajima, M., Terashima, K., Ito, M., Mugishima, H., Fujiwara, S., Shimizu, K., Honda, M., Shimizu, N., and Yamamoto, N. 2007. Humanized NOD/SCID/IL2Rgamma(null) mice transplanted with hematopoietic stem cells under nonmyeloablative conditions show prolonged life spans and allow detailed analysis of human immunodeficiency virus type 1 pathogenesis. *J. Virol.* 81: 13259–13264. [Medline] [CrossRef]

33. Yahata, T., Ando, K., Nakamura, Y., Ueyama, Y., Shimamura, K., Tamaoki, N., Kato, S., and Hotta, T. 2002. Functional human T lymphocyte development from cord blood CD34+ cells in nonobese diabetic/Shi-*scid*, IL-2 receptor γ

null mice. *J. Immunol.* 169: 204–209. [Medline] [CrossRef]

34. Young, G.R., Eksmond, U., Salcedo, R., Alexopoulou, L., Stoye, J.P., and Kassiotis, G. 2012. Resurrection of endogenous retroviruses in antibody-deficient mice. *Nature* 491: 774–778. [Medline]

35. Yu, P., Lübben, W., Slomka, H., Gebler, J., Konert, M., Cai, C., Neubrandt, L., Prazeres da Costa, O., Paul, S., Dehnert, S., Döhne, K., Thanisch, M., Storsberg, S., Wiegand, L., Kaufmann, A., Nain, M., Quintanilla-Martinez, L., Bettio, S., Schnierle, B., Kolesnikova, L., Becker, S., Schnare, M., and Bauer, S. 2012. Nucleic acid-sensing Toll-like receptors are essential for the control of endogenous retrovirus viremia and ERV-induced tumors. *Immunity* 37: 867–879. [Medline] [CrossRef]